On laser beam fluctuations in the surface atmospheric layer during snowfalls

A.F. Zhukov and N.A. Vostretsov

Institute of Atmospheric Optics,
Siberian Branch of the Russian Academy of Sciences, Tomsk

The turbulent component of the radiation scintillation index (β_t^2) for collimated laser beams is used to estimate the structure characteristic (C_n^2) of the air refractive index fluctuations in snowfalls. The β_t^2 component is determined in finely disperse snowfalls from simultaneous measurements of the frequency spectrum and the scintillation index (β^2). The structure characteristic C_n^2 is estimated using only those spectra, which included both the turbulent and hydrometeor maxima with a deep minimum between them. In snowfalls the structure characteristic C_n^2 decreases and does not exceed $4 \cdot 10^{-15}$ cm$^{-2/3}$. No regular interrelation has been found between C_n^2 and the volume scattering coefficient. The scintillation index β^2 increases with the increasing divergence of a narrow laser beam. It does not exceed the maximum value possible in the turbulent atmosphere without precipitation. The probability distribution in a narrow divergent beam is not the lognormal distribution, but the gamma-distribution in the most cases. At low atmospheric turbidity, it is possible to reliably distinguish the haze and precipitation (rain) situations from the spectrum of radiation scattered near the focused beam and the wind velocity. The error of C_n^2 estimation, validity of the used assumptions, and the physical causes for the features observed are discussed.

Introduction

Publications concerning the subject of this paper are far less numerous than those dealing with the laser beam propagation through a turbulent atmosphere without precipitation. However, the measurements in snowfalls and without precipitation have the same goal, namely, to determine the effect of the atmosphere on the characteristics of a laser beam propagated through it. The studies performed earlier of the temporal spectra of fluctuations in snowfalls showed that the turbulence contributes markedly to fluctuations of the received laser signal. It follows from the above-said that it is logical to compare fluctuations measured in snowfalls and without precipitation. The specificity of the studies is that both the turbulence and snowflakes together cause fluctuations of the received laser beam. It is just this poorly studied circumstance that significantly complicates studying the nature of fluctuations and gives rise to uncertainty in analysis of beam fluctuations in snowfalls in connection with the complete absence of the data on turbulence characteristics and precipitation particles. This paper gives an approximate estimate of C_n^2. The importance of the scintillation index of spatial characteristics of a laser beam is demonstrated again from a new point of view.

We present data of tentative experiments on the dependence of the scintillation index in snowfall on the detector's field of view and the temporal frequency spectrum of fluctuations of scattered radiation at low atmospheric turbidity. The experimental probability distributions of laser radiation fluctuations measured in a narrow divergent beam are analyzed. By comparing the published experimental data on fluctuations with no precipitation with our data obtained in snowfall, we show that the worst effect of the atmosphere for a narrow divergent beam (NDB) is possible in the turbulent atmosphere without precipitation.

The techniques for conducting measurements and processing the results can be found, for example, in Ref. 1.

1. Preliminary remarks

Introduce three categories of characteristics. One category includes the quantities that describe the experiments discussed in this paper like the radiation wavelength λ, separation between the source and the detector L (path length), effective size of a Gaussian beam α_0' at the $1/e$ level, total divergence angle θ for NDB, wave front curvature length R_0 at the beam center at the detector, detector diameter D_{det}, detector's field of view γ.

Another one category includes the characteristics that describe the environment during a snowfall. It includes the volume scattering coefficient α, km^{-1}, the maximum size of snowflakes D_{max}, mm, the structure characteristic of the air refractive index fluctuations C_n^2, cm$^{-2/3}$, the inner scale of turbulence l_0, mm, wind velocity V, m/s, and its component normal to the propagation path $V_\perp$, m/s. The third category includes the optical depth τ of the measurement path ($\tau = L\alpha$). In our investigations, the extinction coefficient is

equal to the scattering coefficient. It should be emphasized that the same values of τ can be obtained at variations of both α ($L = $ const) and L ($\alpha = $ const), as well as at an infinite set of different combinations of α and L. Moreover, the same α can be obtained at different particle concentrations with variations of the particle structure, for example, D_{max}. Thus, τ is not an unambiguous characteristic of the medium, and it is illogical to compare fluctuation characteristics at the same τ, but different L, because in this case the comparison is made between data obtained in different media.

This circumstance forced us to systematize measured results in different ways, for example, using α and D_{max}. Let us construct the diffraction parameter of the beam from λ, α_0', and L as $\Omega = k\alpha_0'^2/L$ ($k = 2\pi/\lambda$) and the focusing parameter from L and R_0 as $X = L/R_0$. It is clear that in studying the dependence of the scintillation index on Ω it is preferable to compare data obtained in simultaneous measurements at the same path, but with different Ω.

In the measurements the parameters were the following: $\lambda = 0.63$ μm, $D_{det} = 0.3$ or 0.1 mm. The values of L and θ were used for calculation of the beam size in the detection plane D_P. It coincided with that measured in the experiment. At the output of an LG-38, LG-38A, or LGN-215 lasers, the NDB had the initial diameter of about 4 mm and the total divergence angle $\theta = 10^{-3}$ rad. In all the measurements (except those discussed in Section 4) the detector's field of view was $3.7 \cdot 10^{-2}$ rad (about 2°). In the data presented in Section 4, it varied and was about 10^{-3}, $5 \cdot 10^{-3}$, and $2.7 \cdot 10^{-2}$ rad.

In this paper the fluctuations of laser radiation are characterized by scintillation index β^2, the spectral function $U(f)$, and the probability density $\rho(V')$:

$$\beta^2 \equiv \sigma_I^2 = \langle (V' - \langle V' \rangle)^2 \rangle / \langle V' \rangle^2;$$

$$U(f) = fW(f) / \int W(f)df,$$

where σ_I^2 is the variance of the radiation intensity fluctuations; $W(f)$ is the spectral power density at the frequency f; V' is the signal at the output of a linear amplifier, which receives the signal from a photodetector. Angular brackets $\langle \rangle$ denote time averaging. We averaged β^2 over the interval ≈ 20 s and $U(f)$ over 100 s with each of the filters used. A total of 38 filters were used. The measurement errors in β^2 and $U(f)$ were estimated. As β^2 varied from 0.01 to 1, it did not exceed 15%. For $U(f)$ the amplitude error was within 10%, and the frequency resolution decreased with the increasing frequency and was equal to no less than a half of the separation between the central frequencies of three-octave filters used in an FSP-38 spectrum analyzer.

Fluctuations at the beam axis were measured in 150 snowfalls. However, we did not meet the worst conditions with respect to α, D_{max}, and V that can be observed under natural conditions. Snowfalls have their own features, which should be taken into account in measurements. Every snowfall is individual in the values of physical characteristics and their dynamics. Moreover, almost always in snowfalls, it is impossible to obtain the ensemble of realizations under the same conditions, and in reality, we have to orient at characteristics acquired in a single realization under particular conditions, which are determined only partly.

To improve the quality of measurements, they were accompanied by simultaneous measurements of the atmospheric transmittance made using an RDV-3 device at the 2×100 m path and the wavelength of 0.55 μm. The readouts of the RDV-3 device were used to calculate α and then τ of the measurement path. The wind speed and direction were also measured continuously just near the detector. These findings were used to calculate the wind velocity component normal to the path of the beam propagation. Snowflakes were collected on a fur mat to measure their maximum size D_{max} with a scale rule. The cases of fast variation of τ, D_{max}, and $V_\perp$ were excluded from processing. The criterion of fast variation of the parameters is described in Ref. 5.

From these measurements, we have obtained the data on the basic characteristics of the radiation fluctuations. The features revealed were reported in our earlier publications. Assume that all characteristics of the laser beam fluctuations have the turbulent and snow components denoted by the subscripts "t" and "s," for example, β_t^2 and β_s^2 for the scintillation index β^2 and $U_t(f)$ and $U_s(f)$ for the spectrum $U(f)$.

Then the turbulent β_t^2 and snow β_s^2 components of the fluctuations are assumed independent because of the low concentration of snowflakes in air,[6] that is, $\beta^2 = \beta_t^2 + \beta_s^2$, $U(f) = U_t(f) + U_s(f)$.

2. Estimation of C_n^2 in snowfalls

In fact, not knowing the value of C_n^2, it is impossible to calculate β_t^2 and other turbulent fluctuation characteristics of the beam in the atmosphere without precipitation[3,4,7–10] and in precipitation as well.[2,6,10] In snowfalls C_n^2 is not determined. To find it, we will use measurements in collimated beams at low values of the optical thickness τ (conditions of increasing fluctuations[11,12]). In such measurements the effect of atmospheric turbulence is quite evident. The simultaneous measurements of β^2 and $U(f)$ and the technique described, for the first time, in Ref. 13 and corrected somewhat here are appropriate for achieving our goal. The technique used here, as in Ref. 13, is based on the determination of the area (S) under the curve $U(f)$ in the coordinates $U(f)$ and $\log f$ (corresponding to β^2), as well as the areas S_t and S_s under the turbulent and snow parts of $U(f)$ ($S = S_t + S_s$), which correspond to β_t^2 and β_s^2. As in Ref. 13, S_t and S_s are separated at the frequency f_{min} (Fig. 1).
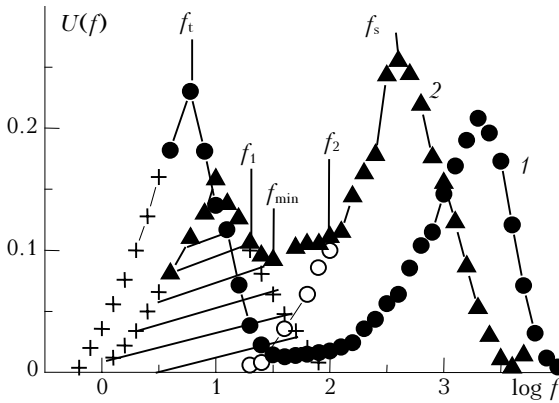
Fig. 1. Spectrum $U(f)$ vs. $\log f$ at $D_{max} < 5$ mm: $L = 130$ m, $\beta^2 = 0.14$, $\beta_t^2 = 0.07$, $\alpha = 0.9$ km^{-1}, $\Omega = 54$ (*1*); $L = 390$ m, $\beta^2 = 0.13$, $\beta_t^2 = 0.05$, $\alpha = 2.1$ km^{-1}, $\Omega = 4.5$ (*2*).

Figure 1 depicts curves *1* and *2* for the best and worst cases with respect to the error in estimation of β_t^2, respectively. To separate the components in β^2, we took not all spectra, but only those satisfying the following two conditions:

1) The difference between the minimum value of $U(f_t)$ and $U(f_s)$ and $U(f_{min})$ normalized to $U(f_{min})$ is greater than 0.5, that is,

$$[U(f_t); \; U(f_s)] \min / U(f_{min}) > 1.5, \qquad (1)$$

where f_t and f_s are the frequencies of the turbulent and snow peaks in the spectrum; f_{min} is the frequency with the minimum value of $U(f)$ between f_t and f_s. Condition (1) means that the function $U(f)$ must have a pronounced minimum between $U(f_t)$ and $U(f_s)$. Condition (1) determines the accepted quantitative measure of such a minimum.

2) Only those spectral curves $U(f)$ are taken, which have the turbulent peak, that is, $U(f) < U(f_t)$. The technique used here differs not only by more rigorous selection of the frequency spectrum $U(f)$, but also by other tricks, namely,

a) the spectrum $U_t(f)$ is extended to intersection with the $\log f$ axis by extrapolating the measured part of $U_t(f)$ (crosses at $f > f_t$ in Fig. 1);

b) then the spectrum of $U_t(f)$ was extended to the left to intersection with the $\log f$ axis (crosses at $f < f_t$, Fig. 1). We have to do this, because the frequency spectrum is measured only in the frequency band from 2 Hz to 20 kHz, while the scintillation index is measured from 0.05 Hz (1/20 s) to 20 kHz. This difference leads to the situation that we ignore a part of the area in S_t, which will be denoted S_+. The spectrum $U_t(f)$ is extended (at $f < f_t$) on the assumption that $U_t(f)$ is symmetric about f_t. The close-to-symmetric spectrum was obtained for weak fluctuations in Ref. 14. It is also presented in Ref. 8 [Fig. 6.37]. The details concerning this aspect are given in Section 8. Open circles in Fig. 1 stand for the snow part $U_s(f)$ obtained as $U_s(f) = U(f) - U_t(f)$ in the area of overlap of the spectra $U_t(f)$ and $U_s(f)$ from f_1 to f_2 (see Fig. 1).

Closed circles and triangles in Fig. 1 are for the measured values of $U(f)$. In our data, we have found 40 spectra with two peaks and a pronounced minimum between them. For the paths of 130, 390, and 650 m long, this makes up to 7% of processed spectra in snowfalls. In the overwhelming majority of spectra, there is no turbulent peak in the frequency range higher than 2 Hz, although the turbulent component in the spectra is clearly seen in the range of low frequencies ($f < f_s$). This is especially characteristic of collimated beams. However, the technique used here fails to estimate this contribution. Addition of the area S_+ to S_t improves the estimate. Emphasize that S_+ in the used spectra is no higher than 36% of S_t.

According to our technique, the maximum error in the S_t estimate consists of two parts. The first one is determined by the ratio of the area under the measured curve $U(f)$ in the frequency range from f_1 to f_2 to the whole area S_t. It is shaded in Fig. 1 for curve *2*. In the spectra used for estimation of C_n^2 this part of the error did not exceed 58%.

The second part of the error is connected with the assumption of the symmetric turbulence spectrum. It was estimated by the ratio of the area under the symmetric curve S_{sym} [Fig. 4.37, Ref. 8] to the area under the whole asymmetric curve S_{asym}, that is, $(S_{sym}/S_{asym}) \cdot 100\%$. This part of the error is roughly equal to 9%. Then the total error in the S_t estimate does not exceed 82% (with the allowance for the measurement error in $\beta^2 \leq 15\%$). The error in S_s was estimated similarly to the estimation of the first part of the error for S_t. In the spectra used it does not exceed 75%.

Estimation of C_n^2 in snowfalls was carried out by the following scheme:

1) The turbulent component β_t^2 was determined from β^2 and $U(f)$ selected by applying the two conditions above.

2) $P_0 = \sigma_\chi^2 / \sigma_{\chi p}^2$ was determined by Fig. 6.1 from Ref. 8 (p. 147) taking into account Ω and L for the collimated beam. Here $\sigma_{\chi p}^2$ is the variance of the log amplitude of a plane wave calculated by the method of smooth perturbations; σ_χ^2 is the same for a beam.

3) From Ref. 4 (p. 538) $\sigma_{\chi p}^2 = 0.308 \, C_n^2 k^{7/6} L^{11/6}$. Then $\sigma_\chi^2 = P_0 \, \sigma_{\chi p}^2 = 0.308 P_0 \, C_n^2 k^{7/6} L^{11/6}$.

4) If the lognormal law is true for turbulent intensity fluctuations in the laser beam in the zone of weak fluctuations[8] and relation from Ref. 4 (p. 396) is valid, we have $\sigma_\chi^2 = 0.25 \ln (\beta_t^2 + 1)$;

5) Then, taking into account that $\lambda = 0.63$ μm, we obtain for C_n^2:

$$C_n^2 = 0.53 \, P_0^{-1} L^{-1.83} \ln (\beta_t^2 + 1) \, k^{-7/6}. \qquad (2)$$

The Table summarizes β^2, β_t^2, α, V, $V_\perp$, and $C_n^2 = P \cdot 10^{-N}$ for $\Omega = 54$, $L = 130$ m, $D_{max} \leq 2$ mm as obtained in nighttime during a long snowfall. In these measurements there is a deep minimum in $U(f)$ between f_t and f_s. In other words, the spectrum components $U_t(f)$ and $U_s(f)$ are actually frequency-

separated. Such spectra can be used for the most accurate estimation of C_n^2.

#	β^2	β_t^2	α, km^{-1}	V, m/s	$V_\perp$, m/s	$C_n^2 =$ $= P \cdot 10^{-N}$, cm$^{-2/3}$	
						P	N
1	0.25	0.06	1.9	6.4	5.5	2.2	15
2	0.22	0.03	1.5	4.6	4.1	1.2	15
3	0.22	0.06	1.3	4.9	4.2	1.9	15
4	0.21	0.05	1.3	5.6	4.8	1.7	15
5	0.21	0.05	1.3	4.6	3.9	1.6	15
6	0.25	0.03	1.3			1.1	15
7	0.31	0.06	1.3	4.2	3.8	1.9	15
8	0.20	0.04	1.2	4.7	4.0	1.5	15
9	0.25	0.04	1.2	5.2	4.5	1.2	15
10	0.13	0.05	1.1	7.4	6.3	1.6	15
11	0.14	0.07	0.9	5.1	4.5	2.4	15
12	0.12	0.06	0.7	3.0	2.7	2.1	15
13	0.14	0.06	0.5	4.6	4.1	2.1	15
14	0.13	0.07	0.5	4.1	3.7	2.4	15
15	0.12	0.08	0.4	3.5	3.1	2.7	15

Figure 2 shows the spectra for measurements 10 and 14 (see the Table) at the same values $\beta^2 \approx 0.13$. Figure 1 (curve *1*) show the spectrum for measurement 11. It follows from Figs. 1 and 2 that the close values of β^2 can be obtained at the $U(f)$ spectra with significantly different shape. Among the variations of the spectral shape, we can separate two characteristic ones. The first one is determined by the ratio of β_s^2 to β_t^2 (or vice versa), while the second one depends on the structure characteristics of snow particles D_{max} and the wind velocity. From β_t^2 estimated in snowfalls occurred on different dates, we calculated the values of C_n^2 for beams with $\Omega = 18$, 4.5, 2.5, and 0.1 at the 390-m path, as well as with $\Omega = 54$ at the 130-m path in eight snowfalls. Each snowfall showed the growth of β^2 and $\delta = \beta_s^2/\beta_t^2$ with increasing α, but no regularity was found in their absolute values.

We assume that this is the influence of the different initial level of turbulence (C_n^2). In the absence of snowflakes, C_n^2 decreases and changes, according to our estimates, from $1.1 \cdot 10^{-15}$ to $4 \cdot 10^{-15}$ cm$^{-2/3}$. In snowflakes β^2 grows and, naturally, β_t^2 increases too (for a more detail see Section 8).
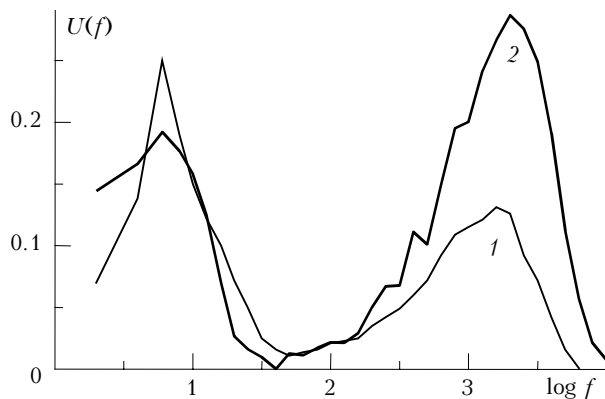
Fig. 2. Spectrum $U(f)$ vs. log f at $D_{max} < 5$ mm: $L = 130$ m, $\beta^2 = 0.13$, $\beta_t^2 = 0.05$, $\alpha = 1.1$ km^{-1}, $\Omega = 54$ (*1*); $L = 130$ m, $\beta^2 = 0.13$, $\beta_t^2 = 0.07$, $\alpha = 0.5$ km^{-1}, $\Omega = 54$ (*2*).

3. Dependence of the mean scintillation index β^2 on the beam diameter at the detection plane D_{det}

Figure 3 shows the dependence $\bar{\beta}^2 = \bar{\beta}^2(D_{det})$ in NDB. The beam diameter in the detection plane in these measurements varied discretely through changes in the source, in which objectives with different focal length (from 25 to 75 cm) were set at the same distance from a laser. This led to a significant change in the laser beam divergence and, naturally, D_{det}.

Figure 3 depicts the dependence $\bar{\beta}^2 = \bar{\beta}^2(D_{det})$ rather than $\bar{\beta}_s^2 = \beta_s^2(D_{det})$. Splitting of β^2 into β_t^2 and β_s^2 is impossible, because $U(f)$ has no pronounced minimum between f_t and f_s. Therefore, we assume $\beta^2 \approx \beta_s^2$, although the contribution of turbulence is evident in the spectra. It follows from Fig. 3 that $\bar{\beta}^2$ increases with the increase of D_{det}, which is in a qualitative agreement with the earlier theoretical[2,6,15,16] and experimental[17,18] results. Moreover, it follows from Fig. 3 that $\bar{\beta}^2$ increases with the increasing maximum particle size D_{max}, as was predicted in Ref. 11 and found in actual snowfalls.[1,12]
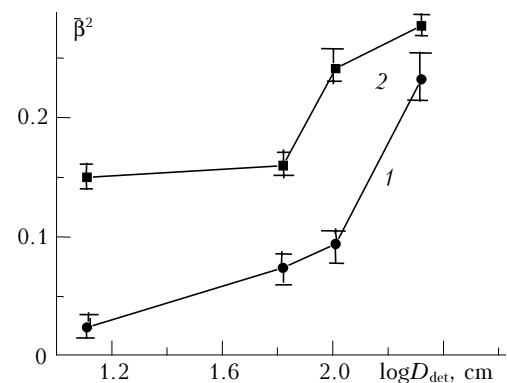
Fig. 3. Mean scintillation index $\bar{\beta}^2$ vs. log beam diameter D_{det} in the detection plane for NDB: $D_{max} = 1$–3 (*1*) and 5–10 mm (*2*), $\alpha = 1$–1.7 km^{-1}. Vertical bars show the spread of β^2 values.

4. Dependence of mean scintillation index β^2 on the detector's field of view γ

We studied the dependence of the mean scintillation index $\bar{\beta}^2$ on the detector's field of view γ. The measurements were conducted in NDB at $\alpha = 0.5$–0.7 km^{-1}, $D_{max} = 1$–3 mm, 130-m long path, and detector's diameter of 0.1 mm. The value of γ was changed by setting diaphragms with different diameters in front of a 1-m long blind placed in front of the photodetector. The mean value of $\bar{\beta}^2$ slightly increases as γ increases from $0.5 \cdot 10^{-2}$ to $2.7 \cdot 10^{-2}$ rad and decreases somewhat as γ decreases ($\gamma = 10^{-3}$ rad). Our explanation of this dependence $\bar{\beta}^2 = \beta^2(\gamma)$ is given in Section 8.

5. Probability distribution in narrow divergent beam

The shape of the empirical probability distribution (EPD) varies considerably. Details concerning this variation can be found in Ref. 22. We continued analysis of EPD. In this section, some new results are presented. We analyzed how the following distributions suit for description of EPD: gamma-distribution, generalized and cutoff gamma-distributions, beta-distribution, normal, lognormal, and exponential distributions.

In analyzing EPD with the right-hand asymmetry, different methods were used: method of rectified diagrams, the least-squares method, method of higher moments, and maximum likelihood method, as well as χ^2 and Kolmogorov–Smirnov criteria. Rare EPD with left-hand asymmetry (40 of 460 EPD) were not studied. They were obtained at simultaneously falling large and small snowflakes. We have a good reason to believe that at the integral probabilities from 0.05 to 0.95 the gamma distribution suits best for describing the EPD. This probability interval is usually used in mathematical statistics. It should be noted that in this interval the gamma-distribution by the χ^2 and Kolmogorov–Smirnov criteria is unsuitable for describing the EPD.

It is especially important that EPD is not described by the lognormal distribution, which works well in the turbulent atmosphere without precipitation[8–10] and in the region of weak fluctuations.

Let us say a few words about the gamma-distribution, whose analytical representation is well known [Ref. 23, p. 192]. For V' the probability density is

$$\rho_{\alpha_0,\,\beta_0}(K_i) = \{(K_i\,\alpha_0/[\Gamma(\alpha_0 + 1)\,\beta^{\alpha_0+1}]\} \times$$

$$\times \exp(-K_i/\beta_0), \qquad (3)$$

where $\alpha_0 > -1$ is the shape parameter; $\beta_0 > 0$ is the scale parameter; $\Gamma(\alpha_0 + 1)$ is the gamma-function (equal to $\alpha_0!$) at integer α_0; $V' \equiv K_i \equiv N_0$, (N_0 is the number of analyzed levels in the pulse analyzer).

The parameter β_0 depends on the amplification factor of the recording instrumentation. As α_0 increases, the gamma-distribution approaches the normal one [Ref. 24, p. 107]. When $\alpha_0 = 0$, the gamma-distribution transforms into the negative exponential distribution [Ref. 24, p. 111]. We obtained the normal distribution at low τ and D_{max} and the negative exponential distribution at high τ and D_{max} [Ref. 22]. Figure 4 depicts the dependence of the gamma-distribution shape parameter α_0 on the optical depth at 260-, 520-, 780-, and 964-m long paths. The values of α_0 were obtained by the method of rectified diagrams using the technique described in Refs. 23 and 25.

Figure 5 refines the variation of α_0 and β^2 for two paths as functions of α and D_{max}, and the tendency in α_0 to decrease with the increasing α is quite obvious.
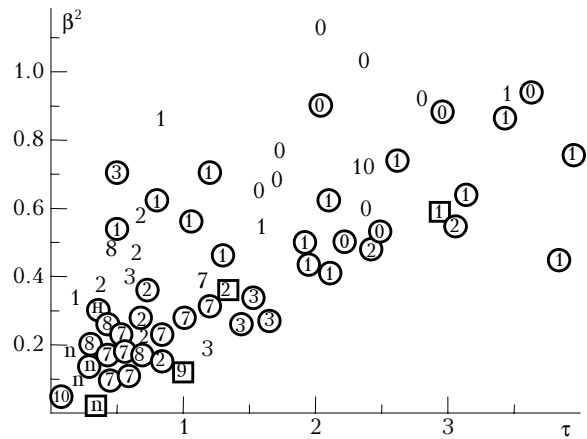

Fig. 4. Gamma-distribution shape parameter α_0 vs. optical depth τ and maximum size of snowflakes D_{max}. Symbol n corresponds to the normal distribution, numbers in circles are for $1 < D_{max} < 5$ mm, numbers in squares are for $D_{max} = 1$ mm, numbers alone are for $D_{max} \geq 5$ mm, and all numbers are the values of α_0.
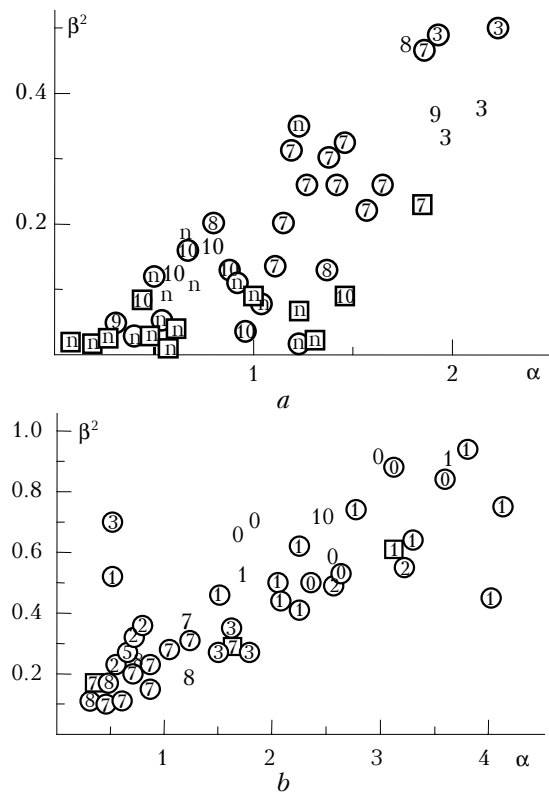

Fig. 5. Gamma-distribution shape parameter α_0 vs. the scattering coefficient α and the maximum size of snow particles D_{max}. Symbol n corresponds to the normal distribution, numbers in circles are for $1 < D_{max} < 5$ mm, numbers in squares are for $D_{max} = 1$ mm, numbers alone are for $D_{max} \geq 5$ mm, and all numbers are the values of α_0. $L = 260$ (a) and 964 m (b).

There is a significant spread in α_0 at the close values of α, which is likely caused by variations of C_n^2 on different measurement days and poor estimation of the particle size distribution, which was roughly determined by only D_{max}. It can be seen from

Fig. 5 that at the 964-m long path and small α the distribution is not normal, while at the 260-m path it is normal. EPD likely depends not only on α, but also on L ($\tau = \alpha L$).

6. Determination of the type of weather at low turbidity of the surface layer of the atmosphere

Objective identification of the existing types of weather in the surface atmosphere at low turbidity is an open problem yet. The meteorological visual range S_{met} is usually used for this purpose. It is obtained from visual observations or from measurements with specialized instruments. However, it is quite clear that the values of S_{met} may be close and even equal in significantly different types of weather, for example, under conditions of a heavy haze (smog) and weak precipitation with rare particles falling (trace precipitation), and in some other cases. It is important that standard precipitation intensity meters do not detect trace precipitation, and optical meters in such cases measure S_{met} with large error and cannot distinguish between the weather types at all.

Uncertainty in solution of the problem about the type of weather decreases, if the measured parameters are fluctuations of scattered optical (laser) radiation. It is better to measure these fluctuations beyond the beam, because at low turbidity of the path by haze or precipitation the turbulence has the decisive effect on fluctuations of the detected radiation. Therefore, to get rid of this effect, it is worth removing the photodetector from the beam. It can be set at any angle to the beam, but it is desirable to take a rather large volume, from which the scattered radiation is received, in order to decrease the effect of fluctuations in the concentration of scattering particles, and the detector should not strongly suppress fluctuations. It is also worth taking the wavelength shorter than the size of scattering particles.

By the reasons known from atmospheric optics, the smallest scattering angles (beyond the beam) are preferable. Almost all requirements to the detector are met when using a focused optical beam from a He–Ne laser. In this case, the beam has the smallest size near the photodetector, which allows measuring only scattered radiation within extremely small scattering angles (near the beam) with the highest intensity of the scattered radiation and using a small-size detector operating in the current mode even at the laser power of tens of mW. Unlike the existing techniques measuring the mean signal, our technique assumes measuring signal fluctuations normalized to the mean measured signal, thus significantly decreasing the measurement errors connected with the imperfection of optical parts forming the laser beam, and this provides the possibility of measuring within extremely small scattering angles.

So, we have measured the basic characteristics of fluctuations of the received scattered radiation of a focused laser beam at the 130-m path in haze, drizzle, rain, and snow at very low turbidity ($S_{met} > 5$ km) at the distance $\Delta l = 1$ cm from the beam axis. (We do not know any other similar atmospheric experiments.) The beam diameter in the detection plane was roughly equal to 0.4 cm, $\Omega \approx 54$. The diameter of the receiving diaphragm set in front of a photomultiplier tube was equal to 0.1 mm, and the total detector's field of view was $\gamma = 3.7 \cdot 10^{-2}$ rad. First, the photodetector unit along with the blind was set at the optical axis of the focused beam. Then the detection angle and the blind were displaced by microscrews in parallel by 1 cm away from the optical axis of the focused beam. Other details of the measurements were described in Refs. 26–28, where the dependence of β^2, $U(f)$, and $\rho(V')$ on τ and $V_\perp$ was analyzed.

We studied the dependence of δ' on V and $V_\perp$: $\delta' = f_{max}/V$ or $f_{max}/V_\perp$, where f_{max} is the frequency of maximum in a haze or $f_{max} \equiv f_s$ in precipitation. It turned out that the ratio $f_{max}/V_\perp$ carries little information, while $\delta' = f_{max}/V$ is different for rain and haze, and δ' can be used to reliably distinguish haze and rain. We failed to distinguish drizzle and snow from haze, drizzle from rain, and rain from snow, because the rates of gravitational fall of haze, drizzle, and snowflakes are rather close. In rain and haze, the rates of gravitational fall of particles differ widely, and this allows us to distinguish between the rain and haze situations. Therefore, at strong wind it is necessary to measure not only the spectral maximum and the wind velocity, but also the rate of gravitational fall of particles.

The proposed method is not ideal, because mistakes are possible in selection of the instrumentation. The values of V can be measured by standard meteorological equipment. So our task is reduced to measurement of the position of maximum in the frequency spectrum. The increase of the scattered radiation flux in the proposed method improves the capabilities of the measurement instrumentation, which is one of its benefits. Moreover, the dynamic properties of the scattered radiation in the atmosphere vary in a wide frequency range, and at proper organization of measurements, they bear information about the type of weather.

7. Comparison of scintillation index and frequency spectrum in snowfalls and in the atmosphere without precipitation

Let us start from the normalized scintillation index. For a comparison, take the data from Ref. 19 [Fig. 4] ($\lambda = 0.43$ μm, Gaussian laser beam, $L = 1200$ m, beam diameter of about 20 mm at the entrance into the atmosphere (at e^{-2} level), total divergence of $3.9 \cdot 10^{-3}$ rad, path altitude of 1.2 m, diameter of the receiving diaphragm of 0.25 mm). In Ref. 19 the conditions of propagation along the path were described using C_n^2, l_0, and $V_\perp$. These three parameters were simultaneously measured with optical

devices at the paths near the principal one. Such measurements were conducted, likely, for the first time. They significantly improve the quality of the experiment. In Ref. 19 the maximum values of β^2 were obtained in the so-called focusing mode. The spread of β^2 in Ref. 19 was largely determined by different vales of l_0 occurred in measurements.

Figure 6 shows β^2 (AD scale) as a function of β_0^2 (DC scale) in the turbulent atmosphere without precipitation from Ref. 19 [Fig. 4] and β^2 (CB scale) as a function of τ (AB scale) at $L = 37 - 1928$ m, $D_{max} \le 5$ mm, $D_{det} = 0.1$ mm in snowfall in NDB with the divergence of 10^{-3} rad. It should be emphasized that the AD scale is tenfold as large as the BC scale. The domain of variability of β^2 as a function of τ lies between the solid curves. The domain of variability of β^2 as a function of β_0 is shown by dashed curves. It follows from Fig. 6 that the maximum fluctuations in NDB in snowfall ($D_{max} \le 5$ mm) are roughly eightfold as low as those in a quasispherical wave[19] without precipitation. The spread of β^2 values in snowfall is caused by variations of D_{max} and, possibly, l_0. It should be also noted that in collimated beams the maximum value of β^2 we measured at a 1310-m long path ($\Omega = 8.5$) was $\beta^2 \approx 1.1$, which is roughly sixfold as low. At a 390-m long path ($\Omega = 4.5$) in a weak snowfall β^2 was a little bit higher than unity (sleet $D_{max} \le 3$ mm). In all other cases of a collimated beam $\beta^2 < 1$. However, in NDB at a 650-m path in heavy flakes ($D_{max} \approx 7$ mm) the measured values of β^2 achieved 1.7 [Ref. 1], which is still fourfold as low as compared with possible turbulent fluctuations without precipitations.
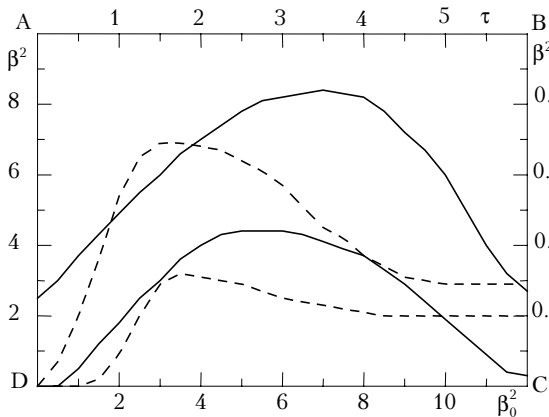

Fig. 6. Dependence of β^2 (AD scale) on $\beta_0^2 = 0.496\, C_n^2 \kappa^{7/6} L^{11/6}$ (DC scale) without snow and dependence of β^2 (BC scale) on the optical depth τ (AB scale) in snowfall in NDB. ($L = 37 - 1928$ m, $D_{max} \le 5$ mm, $D_{det} = 0.1$ mm).

Let us now compare the frequency spectrum. Curve *1* in Fig. 7 shows the highest-frequency spectrum from Ref. 20 obtained without precipitation. It was measured at a path with $L = 1750$ m ($\lambda = 0.63$ μm, collimated beam with the output diameter of 50 cm). The wind velocity ($V_\perp$) was not measured in Ref. 20, but it is likely higher than 6.5 m/s.
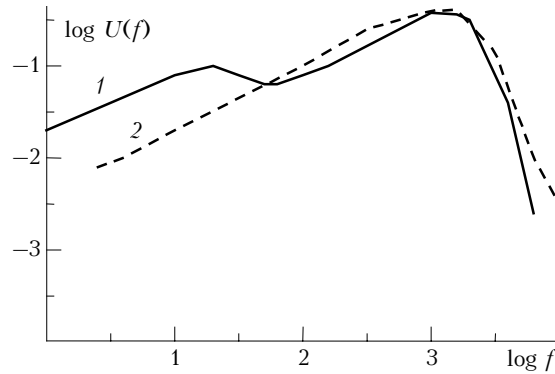

Fig. 7. Dependence of log $U(f)$ on log f: without precipitation, Ref. 20 (curve *1*) and in snowfall, Ref. 21 (curve *2*).

Curve *2* in Fig. 7 corresponds to the highest-frequency spectrum obtained in snowfall.[21] It was measured in NDB at a 130-m path with $\alpha = 5.6$ km^{-1} and the wind velocity of 12 m/s ($V_\perp = 6-7$ m/s), $D_{max} \le 5$ mm. The frequency spectrum in snowfall may be comparable with or somewhat higher (in frequency) than the spectrum of strong turbulent fluctuations. However, according to our data, usually the spectrum in snowfall has lower frequencies as compared to the highest-frequency spectrum in the region of strong fluctuations.[20]

Thus, it is clear that maximum temporal distortions of a laser signal are possible in the turbulent atmosphere without precipitation. This is one of the main results of this investigation.

8. Discussion

The most part of the results reported in this paper can be explained based on the concepts known in atmospheric physics and optics, we failed to construct the general pattern of all features of fluctuations. For example, we failed to explain logically why the dependence of β_s^2 on D_{max} is not always true in a collimated beam. This is especially strange, since such dependence in NDB is regular and experimentally observed. The enhanced role of turbulence in fluctuations at insufficiently accurate separation of β_t^2 and β_s^2 likely weakens the anticipated dependence in some cases. So, further measurements with more careful separation of the components of fluctuations are needed in this part of the problem. Further measurements of fluctuations are also needed to study the dependence $\beta_s^2 = \beta_s^2(\gamma)$ in a wider range of γ.

Daytime measurements were usually conducted under overcast conditions, when the influx of the solar energy to the snow surface was low, which decreased C_n^2 as compared to the fine weather. At night C_n^2 is usually lower than in daytime, and the effect of clouds on C_n^2 is weaker. We also measured the vertical temperature gradient with temperature sensors set at the heights of 1 and 3 m (or 0.5 and 2 m). The sensors were well protected against snow. The temperature gradient gradually decreased in time down to zero (with regard for the measurement error), likely, due to snow present in the air. The mean separation between snowflakes is far larger than the thickness of the

boundary layer on a particle surface and, in addition, particles move downward independently of each other. So in snowfall there is no directed downward heat flux, although particles are deposited onto the surface. Snowflakes change only the temperature of the upper layer of the snow surface and cause gradual change of the vertical temperature gradient in air because of the different thermal inertia of air and the snow surface. We failed to find in the literature quantitative estimates of such changes.

In estimating C_n^2, we had to accept some assumptions, whose validity is, to put it mildly, quite questionable. They are listed below with brief comments.

1. The turbulent and snow components of fluctuations are assumed additive. This is not proved experimentally yet. In the theory there is no common opinion about this. It is clear from the spectra that in the frequency range from f_1 to f_2 (S_{ov} is the overlap area) the spectra $U_t(f)$ and $U_s(f)$ overlap. The significance of S_{ov} in S_t and S_s is high. It varies in time and determines the value of the maximum error in estimation of C_n^2, especially, at low values of S_t. Moreover, the frequencies f_1 and f_2 are selected without rigorous physical reasoning, but based on the characteristic slope of the measured part of $U(f)$, which inevitably causes some subjectivity in solution. Additivity of the components of fluctuations simplifies the problem, but it is still questionable and calls for rigorous justification.

2. Measurements are conducted in the region of weak turbulent fluctuations. This assumption is valid, since usually the measured $\beta^2 < 1$.

3. We calculated σ_χ^2 from β_t^2 on the assumption that the turbulent component of the intensity fluctuations in snowfall is distributed by the lognormal law. Here $\chi = \ln A$, A is the electric field amplitude. This is not proved experimentally. The lognormal law is acceptable, in particular, for laser beams in the region of weak fluctuations without precipitations. In snowfalls, fluctuations are not distributed by this law, but this is true for the mixture of two components. In our opinion, nothing hampers the fulfillment of the lognormal distribution for one turbulent component of fluctuations in snowfalls.

4. All turbulent fluctuations were attributed to C_n^2, which is not rigorously true, as shown by the data from Ref. 19. Some of them are caused by the inner scale of turbulence (l_0). The value of l_0 in snowfalls is undetermined, and it is impossible to qualitatively assess the overestimation of C_n^2.

5. The assumption that the turbulent part of the spectrum in snowfall is symmetric contradicts the theoretical calculations,[4,8–10] but the experimental spectra measured[4,8,14] in a wide frequency range, including low frequencies ($f < 2$ Hz), are close to symmetric in the vicinity of the maximum. Asymmetry increases at $U(f) < 0.2$. This range of $U(f)$ values is significant in our spectra. Our estimate based on the spectrum for weak fluctuations [Ref. 14, Fig. 4.37] and the assumption of spectrum symmetry suggest that we lose ~ 9% of area when estimating S_t. Then the total error in estimation of S_t is no more than 82% with regard for the 15% error in measurement of β^2. So, C_n^2 is estimated with a large error.

6. The capabilities of the method used here for estimation of C_n^2 in snowfalls are also restricted by the fact that the scintillation index β_s^2 increases with the increasing particle size (D_{max}). This is characteristic of NDB[1,12] and not still proved experimentally for all our data for collimated beams because of the interfering effect of turbulence. The effect of D_{max} is weakened, because C_n^2 is estimated from measurements with $D_{max} \leq 1–5$ mm, that is, with no flakes. The dependence $\beta^2 = \beta^2(D_{det})$ follows from the theoretical calculations in Ref. 2 and other papers. The increase of β^2 with the growth of D_{det} at a point source with a finite detection angle is likely caused by the increasing role of particles lying beyond the laser beam axis, near which the detector is set, in fluctuations of the signal. It is just this factor that also causes variation of $\bar{\beta}^2 = \bar{\beta}^2(\gamma)$. Of particular importance here is the relation between γ and λ/D_r, where D_r is the mean particle diameter. The dependence $\bar{\beta}^2 = \bar{\beta}^2(\gamma)$ should clearly manifest itself at $\gamma < \lambda/D_r$ [Ref. 29].

7. A question inevitably arises: what does affect $\bar{\beta}^2$: $X = L/R_0$ or D_{det}, or, perhaps, X and D_{det} simultaneously? The effect of X was determined experimentally in Ref. 18, while the role of D_{det} was demonstrated in Section 3 of this paper. Formally, X and D_{det} are related to each other, and this relation is uncertain. The answer to the above question mostly depends on whether the volume scattering coefficients depends on X and D_{det}. This is especially important for a laser beam in snowfall, when the beam cross size is comparable with or smaller than the particle size. Such a case is possible in snowfall with flakes in NDB near a detector and in a focused beam near the focal point. The optimal way to find the answer to the above question is to measure simultaneously fluctuation characteristics at equal D_{det}, but essentially different X.

Let us say a few words about f_t. The values of f_t change only slightly in snowfall at significant variations of $V_\perp$. We cannot explain this feature. This is, possibly, caused by changes in the turbulence spectrum in snowfall that were not monitored experimentally or by the insufficient number of measurements in the frequency range near f_t.

Among all the variety of measurements, a particular attention should be paid to the measurements with different Ω at the same (130-m or 390-m long) paths. In these measurements the same conditions are automatically realized for different beams, namely, at the 130-m path in the collimated beam $\Omega = 54$ and in NDB $\Omega = 7.5 \cdot 10^{-2}$; at the 390-m path in the collimated beam $\Omega = 4.5$ and 2.5 and $\Omega = 18$ and 0.1. In all the three cases, β^2 is lower at smaller Ω, which agrees qualitatively with the calculations for a coarse-disperse scattering medium without turbulence, as well as with the turbulent atmosphere without precipitation in the region of weak fluctuations.

The shape of the empirical probability distribution (EPD) in snowfall varies and depends on the relation

between the contributions to fluctuations coming from turbulence and precipitation. Their role changes considerably depending on the snowfall intensity, particle size, and beam parameters. To determine these dependences, multiversion measurements are needed at close (or, better, identical) medium characteristics, which are quite rare in practice, so uncertainties in the dependences are inevitable. In Sections 3, 4, and 5, we have considered only NDB and thus restricted the problem, which allowed us to find a particular solution.

In our opinion, the gamma-distribution is preferable, since it well describes most of the observed dependences in EPD at variation of its shape parameter (α_0) from 0 to 15, although it should be emphasized that we failed to find a physical explanation to the gamma-distribution. Some reasoning concerning this subject can be found in Ref. 22.

We have demonstrated experimentally the possibility of determining, in principle, the type of weather at low turbidity of the surface atmosphere by measuring the frequency of the maximum of the scattered radiation near a focused laser beam and the wind velocity. The practical need in such a meter is still urgent; we are developing a simplified version of a meter.

The results of comparison are quite illustrative and, in our opinion, do not require additional comments. For the comparison made, we took the results available for the turbulent atmosphere without precipitation, which are largely confirmed by theoretical calculations. Therefore, the comparison of our data in snowfall with the results obtained theoretically for turbulent media can hardly give new information.

Conclusions

1. The structure characteristic of the refractive index fluctuations (C_n^2) in snowfall without flakes decreases and, according to our data, does not exceed $4 \cdot 10^{-15}$ cm$^{-2/3}$.

2. The scintillation index in a narrow divergent beam increases with the increasing beam divergence.

3. The lognormal distribution fails to describe EPD, while the gamma-distribution suits best for describing the empirical probability distributions of a laser signal in a beam.

4. The maximum random modulation depth of the laser beam radiation intensity in the atmosphere without precipitation exceeds that in snowfalls.

5. The maximum fluctuation frequency in snowfalls is comparable with or somewhat higher than that in the turbulent atmosphere without precipitation.

6. At low atmospheric turbidity, haze and rain situations can be reliably distinguished based on the spectrum of the scattered radiation and the wind velocity.

Acknowledgments

References

1. A.F. Zhukov and N.A. Vostretsov, Atmos. Oceanic Opt. **9**, No. 8, 670–676 (1996).
2. V.A. Krutikov, Izv. Vyssh. Uchebn. Zaved., Radiofiz. **23**, No. 12, 1434–1446 (1980).
3. A.S. Monin and A.M. Yaglom, *Statistical Fluid Mechanics: Mechanics of Turbulence* (Nauka, Moscow, 1900), Parts 1 and 2, pp. 1965–1967.
4. V.I. Tatarskii, *Wave Propagation in a Turbulent Medium* (McGraw-Hill, New York, 1961).
5. A.F. Zhukov and N.A. Vostretsov, Atmos. Oceanic Opt. **13**, No. 11, 962–969 (2000).
6. V.A. Krutikov, in: *Problems of Atmospheric Optics* (Nauka, Novosibirsk, 1983), pp. 141–150.
7. R.S. Lawrence and J.W. Strohbehn, Proceedings of the IEEE **58**, No. 10, 130–153 (1970).
8. A.S. Gurvich, A.I. Kon, V.L. Mironov, and S.S. Khmelevtsov, *Laser Radiation in the Turbulent Atmosphere* (Nauka, Moscow, 1976), 275 pp.
9. V.L. Mironov, *Laser Beam Propagation in the Turbulent Atmosphere* (Nauka, Novosibirsk, 1981), 246 pp.
10. V.E. Zuev, V.A. Banakh, and V.V. Pokasov, *Optics of the Turbulent Atmosphere* (Gidrometeoizdat, Leningrad, 1988), 270 pp.
11. A.G. Borovoi, Izv. Vyssh. Uchebn. Zaved., Radiofiz. **25**, No. 4, 391–400 (1982).
12. A.F. Zhukov, Atmos. Oceanic Opt. **6**, No. 1, 19–21 (1993).
13. A.F. Zhukov and R.Sh. Tsvyk, Izv. Akad. Nauk SSSR, Fiz. Atmos. Okeana **16**, No. 2, 164–171 (1980).
14. A.S. Gurvich and V.V. Pokasov, Izv. Vyssh. Uchebn. Zaved., Radiofiz. **16**, No. 6, 913–917 (1973).
15. I.P. Lukin, *"Light wave fluctuations in the scattering medium. Gaussian beam,"* Dep. VINITI, No. 2551–78 (1978), 33 pp.
16. V.L. Mironov and S.I. Tuzova, Izv. Vyssh. Uchebn. Zaved., Radiofiz. **23**, No. 12, 1453–1463 (1980).
17. A.F. Zhukov, M.V. Kabanov, and R.Sh. Tsvyk, Izv. Akad. Nauk SSSR, Fiz. Atmos. Okeana **21**, No. 2, 147–153 (1985).
18. A.F. Zhukov, R.Sh. Tsvyk, and N.A. Vostretsov, Opt. Atm. **1**, No. 4, 30–35 (1988).
19. A. Consortii, F. Cochetti, S.H. Churnside, and R.I. Hill, J. Opt. Soc. Am. A **10**, No. 11, 2354–2362 (1993).
20. A.S. Gurvich, R.A. Kazaryan, S.O. Lomadze, K.P. Pogosyan, and V.V. Pokasov, Izv. Vyssh. Uchebn. Zaved., Radiofiz. **18**, No. 4, 610–613 (1975).
21. V.N. Galakhov, A.V. Efremov, A.F. Zhukov, V.V. Reino, and R.Sh. Tsvyk, Izv. Akad. Nauk SSSR, Fiz. Atmos. Okeana **12**, No. 12, 1251–1260 (1976).
22. N.A. Vostretsov and A.F. Zhukov, Atmos. Oceanic Opt. **8**, No. 12, 997–1003 (1995).
23. L.M. Levin, *Research into Physics of Coarse-Disperse Aerosols* (AN SSSR, Moscow, 1961), 267 pp.
24. G.J. Hahn and S.S. Shapiro, *Statistical Models in Engineering* (Wiley, New York, 1967).
25. N.A. Vostretsov and A.F. Zhukov, Atmos. Oceanic Opt. **16**, No. 1, 35–37 (2003).
26. N.A. Vostretsov and A.F. Zhukov, Atmos. Oceanic Opt. **7**, No. 1, 12–14 (1994).
27. N.A. Vostretsov and A.F. Zhukov, Atmos. Oceanic Opt. **12**, No. 8, 660–664 (1999).
28. N.A. Vostretsov and A.F. Zhukov, Atmos. Oceanic Opt. **12**, No. 12, 1111–1112 (1999).
29. J.R. Clark, J.R. Baird, and R.S. Reardeh, Appl. Opt. **15**, No. 2, 314–315 (1976).